ISSN: 2634-9221
European Journal of Applied Sciences; Vol. 14 No. 02 (2026) (75-99)
https://doi.org/10.14738/aivp.1402.19970

Application of Aeromagnetic Data to Assess the Structures, Mineralisation-Porphyry Systems and 2D Modelling of Parts of Northwest Nigeria

Akpaneno, A. F. & Abdullahi, H. A.

1. Department of Geophysics, Federal University Dutsin-Ma, Katsina, Nigeria

Abstract: This study takes a close look at high-resolution aeromagnetic data to map out structures, porphyry-style mineralization systems, and the basement configuration in parts of northwestern Nigeria, specifically the Maru, Anka, and Zuru schist belts, along with the nearby Sokoto Basin. The total magnetic intensity data was processed through upward continuation and reduced to the pole, then enhanced using various techniques like analytic signal, first vertical derivative, the application of 3D Euler deconvolution and the Centre for Exploration Targeting (CET) structural and porphyry plug-ins. We constructed three 2D magnetic models along profiles across the basin margin using GM-SYS to better understand the basement relief beneath the sedimentary cover. The analytic signal and first vertical derivative maps effectively distinguish a weakly magnetic sedimentary area in the west from a strongly magnetic basement terrain in the east, revealing major lineaments that primarily trend WNW-ENE, NE-SW, NNE-SSW, and NW-SE. The CET structural density mapping points out zones with high and very high structural densities, while the CET porphyry analysis identifies circular to subcircular magnetic centres that align with these structurally complex areas. Euler solutions suggest that most depth ranges in the basement sector are shallower than 450 m, with some deeper solutions found beneath the sedimentary basin. The 2D models indicate sediment thickness ranging from about 0.55 to 1.2 km over a gently undulating crystalline basement. The combined results highlight several structurally prepared, alteration-related targets that show promise for gold and Pb-Zn mineralization in both the schist belt basement and the Sokoto Basin margin.

Keywords: High-resolution aeromagnetic data, Sokoto Basin, Maru-Anka-Zuru schist belts, porphyry-style mineralization, gold and Pb-Zn mineralization

INTRODUCTION

Aeromagnetic survey is a strong, rapid, cost-effective, and versatile geophysical approach for identifying subsurface geological structural lineaments. This capability arises because aeromagnetic data can detect changes in the magnetic field caused by changes in magnetite within the constituent rocks (Suleiman, 2025; Faruwa *et al.*, 2021; Lawa *et al.*, 2021; Salawu *et al.*, 2020; Gafaar, 2015 and 2012; Ge *et al.*, 2020). For several decades, the airborne magnetic method has been applied worldwide to delineate structure within the basement, which is a prevalent feature that controls ore mineralization (Ohaegbuchu *et al.*, 2025; Gaafar, 2015; 2014; Faruwa *et al.*, 2021). It has also proven effective in mapping geologic structures associated with orogenic gold deposits (Olomo *et al.*, 2022a).

Structural features such as faults, joints, shearing, and fractures originating from tectonic processes and hydrothermal fluid migration have been successfully employed as efficient indicators in the characterization of ore bodies (Li *et al.*, 2025; Guo *et al.*, 2024; Chang *et al.*, 2024; Han *et al.*, 2024; Pan *et al.*, 2023; Sternberg, 2023; Yang *et al.*, 2023;

Guillou-Frottier *et al.*, 2023; Zhao, 2023). These structures play vital roles in the mobilization, concentration, and emplacement of major gold deposits. Structures are essential in mineral ore exploration, groundwater evaluation, geothermal research, warm spring analysis, and dam design, as they facilitate the movement of hydrothermal fluids within the subsurface (Maarifa *et al.*, 2024; Liu *et al.*, 2024; Dou *et al.*, 2024; Gadge *et al.*, 2023). The deduction of the presence of mineral ore in an environment is done by identifying the characteristics of magnetic anomaly responses to structures that host minerals (Fedi, 2002; Ohaegbuchu *et al.*, 2025; Schwarck *et al.*, 2025; Heincke *et al.*, 2025; Li *et al.*, 2025;). In mineral exploration, particularly within hydrothermal alteration terrains, magnetic data is used to accentuate structural regimes and delineate suitable pathways that may have facilitated hydrothermal fluid circulation and subsequent mineral accumulation (Tulepbayev and Tulemissova, 2025; Kang and Guan, 2025; Ohaegbuchu *et al.*, 2025). An ore can be identified by the environment of its emplacement (deposition) or by noting the pattern of alteration, which is a way of assessing responses to mineralization within hydrothermal alteration zones (Mindiashvili *et al.*, 2025; Zaccarini *et al.*, 2025). As put forward by Zaccarini *et al.* (2025), and Kang and Guan (2025), hydrothermal alteration produced an outstanding magnetic response feature that is far different from geological fabric that has not been affected by hydrothermal alteration. Given the significant structural influence on the distribution of magnetic minerals, airborne magnetic data has become one of the most widely used tools for uncovering subsurface geological structures linked to mineralization (Ohaegbuchu *et al.*, 2025). When integrated with complementary geoscientific approaches, magnetic datasets have successfully revealed subsurface evidence of mineralization, alteration zones, and structurally controlled targets (Tulepbayev and Tulemissova, 2025; Kossov *et al.*, 2025; and Shi *et al.*, 2025). The occurrence of ore minerals in Nigeria has long been understood to be controlled by geological structures that act as conduits for mineralization fluids, allowing them to solidify within the host rock (Ohaegbuchu *et al.*, 2025; Idriss, 2025).

Nigeria's rich mineral resources occur throughout the country, most of which are found within the northwest and southwest portions of the country in the schist belts (Narimi *et al.*, 2025; Alabi *et al.*, 2025; Usman *et al.*, 2025; Ganiyu *et al.*, 2025; Emumejaye *et al.*, 2025; NGSA, 2006). These schist belts consist of metamorphosed sedimentary rocks and low-grade volcanic formations that have experienced deformation, making them ideal candidates for hosting mineral systems that are controlled by structural features (Suleiman, 2025; Ugwu and Ekwueme, 2025; Adebayo *et al.*, 2025).

Numerous studies have examined the Nigerian Western Schist Belt to identify structural features and hydrothermal alteration zones linked to gold mineralization. (Adejuwon *et al.*, 2025; Suleiman, 2025; Okpoli *et al.*, 2025; Manekator and Aigbedion, 2025; Oghonyon and Nnurum, 2025; Ogah and Abubakar, 2024; Akinlalu, 2023; Augie *et al.*, 2024; Salako *et al.*, 2024; Augie *et al.*, 2022a; Augie *et al.*, 2022b; Umaru *et al.*, 2022; Aliyu *et al.*, 2021; Arogundade *et al.*, 2021). Suleiman *et al.* (2025) used aeromagnetic data to delineate structures linked to gold mineralization in northwest Nigeria. Narimi carried out integrated aeroradiometric and XRF techniques to map mineralized and hydrothermally altered zones in Zamfara and its surrounding areas. Okpoli *et al.* (2025) integrated geological, geophysical, and geochemical methods to characterize gold mineralization at Owu in the Kushaka-Kusheriki schist belt. Umaru *et al.* (2022) used aeromagnetic and aeroradiometric data to map lithology, structures, and hydrothermal alteration zones in

Kaiama, NW Nigeria, targeting gold mineralisation. Also, Aliyu *et al*. (2021) used airborne magnetic and radiometric data to investigate gold-hosting structures in the Bida Basin and Zungeru-Schist Belt, Niger State. Adejuwon *et al*. (2025) integrated airborne magnetic, radiometric, and ground geophysical surveys to identify linear structures in Birnin Gwari, NW Nigeria, interpreted as potential ore-hosting veins. Salako *et al*. (2024) analyzed airborne magnetic and radiometric data to map gold potential zones in southern Kebbi State, Nigeria. Also, Augie *et al*. (2022a) analyzed high-resolution aeromagnetic data to delineate gold-hosting structures in the middle parts of the Anka Schist Belt. Augie *et al*. (2022b) also mapped magnetic signatures in southern Kebbi State to delineate structures potentially hosting gold mineralization. Most of the reviewed studies focus on structurally controlled gold within schist belts, with limited attention to porphyry-style mineralization systems. Porphyry-related magnetic signatures (e.g., concentric patterns, magnetite halos) are not specifically targeted or interpreted. Hydrothermal alteration was assessed via radiometric methods, with minimal use of magnetic destruction zones. Porphyry systems are absent. There's a lack of integration between magnetic data, alteration zoning, and porphyry diagnostics for precise gold targeting, and all these are applied in this study.

The research on the sedimentary section in this study area is still quite underdeveloped, as most existing studies have mainly concentrated on the basement complex. As a result, we lack clarity on the geometry, depth, and internal structure of the sedimentary cover, largely due to our insufficient use of quantitative geophysical modelling. These shortcomings underscore the need for a more sophisticated, high-resolution geophysical study that focuses on (i) accurately mapping structural features, (ii) characterizing porphyry intrusions, and (iii) performing 2D modelling of the sedimentary section to enhance our understanding of its subsurface layout and mineralization potential.

LOCATION, GEOLOGY AND TECTONIC SETTINGS OF THE STUDY AREA

Location

The research area is a rectangular block that is in northwest Nigeria, encompassing portions of the Basement Complex and the Sokoto Basin (Figure 1). The research region is located within sections of the northwestern Nigerian schist belts. It is bounded by latitudes 04° 30′ N and 06° 30′ N and longitudes 11° 00′ E and 12° 30′ E (Figure 2). The research area encompasses the northwest of Tambawa in the northwestern section, the northeastern region of Maru in the northeast, the southwestern area of Lumu in the southwest, and the southeastern vicinity of Dan Gulbi in the southeast. The area predominantly encompasses Zamfara State and somewhat extends into the southern regions of Sokoto State and Kebbi State. The topography or elevation within the research area, as shown by the analysis of SRTM data, varied from 179 m to 637 m above sea level. Regions of high elevation are in the east, and places of low height above sea level are found in the west. Settlements such as Tungan-Rihi, Jigawa, Tokwatcho, Bawada, Guma, Mallamji, and Saula have low relief, while Dan Gulbi, Bindim, Gidan Garba, Ben, Maru, Karaka, and Badaku have high relief.

Geology and Tectonic Settings

The study area comprises both basement and sedimentary formations and is tectonically located within the Pan-African mobile (Wright, 1985). The sedimentary section represents

the southern boundary of the Iullemeden basin, also known as the Sokoto basin. Abaa (1983) posited that the deformational event known as the Pan African transpired in this region, leading to regional metamorphism and the development of migmatite, granite, and gneiss. The basement complex of Nigeria has been classified into three units (Obaje, 2009), which are the Migmatite-Gneiss Complex, Schist Belts, Older Granites, and Undeformed Acid and Basic Dykes. The Schist Belts are a region in Nigeria characterized by low-temperature metamorphosed sediments, orientated in a north-south direction in the northwest of the country. The rocks are Upper Proterozoic in age and are associated with the MG complex. Certain rocks may harbor relics of the ocean floor in minor back-arc basins. Grant (1978) posits the existence of multiple basins of deposition, although McCurry (1976) interprets the schist belts as vestiges of a singular supracrustal layer. Both individuals regard these rocks as having originated from faulted rift-like structures.

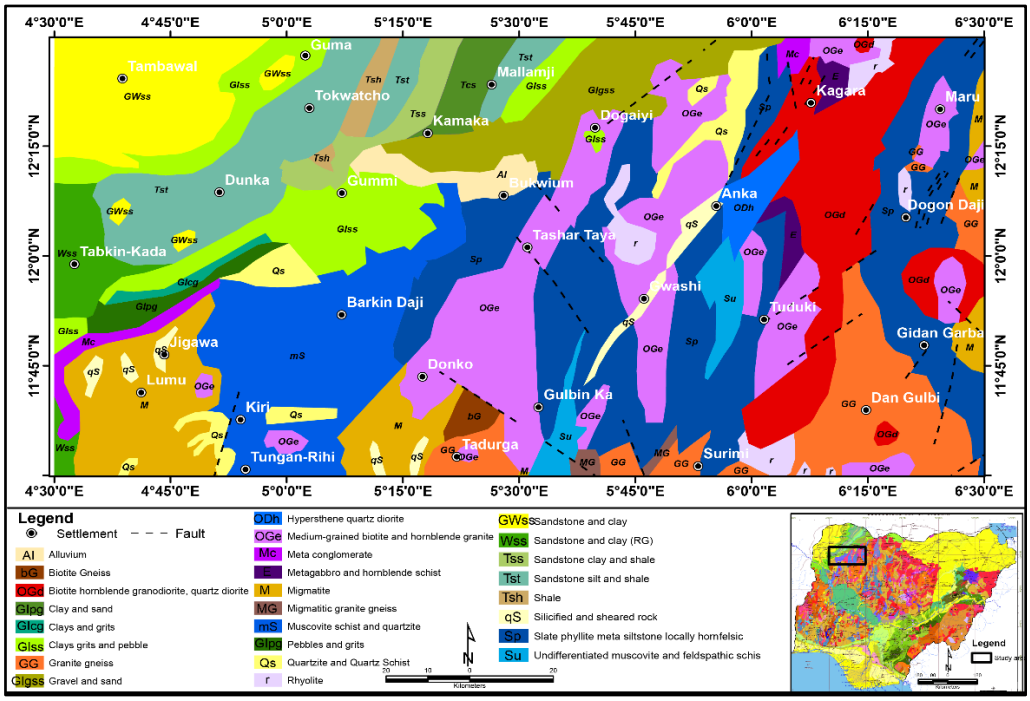

Figure 1: Location and Geologic Map of the Study Area (Modified from NGSA, 2006)

Turner (1983) asserts that sediment ages fluctuate based on structural and lithological correlations. Ajibade *et al*. (1979) contest this finding, illustrating that both series experienced identical deformation histories. Truswell and Cope (1963) regarded the structural connections between the schist belts and the basement as conformable metamorphic fronts, while Ajibade *et al*. (1979) were the pioneers in identifying structural discontinuity. Figure 1 illustrates the rock units within the research region. The dates of the Individual rocks found within this ecosystem are still problematic; however, the older granites showed a bottom limit to be 750 Ma. The ages of the amphibolite complexes inside these rocks have also stirred controversy. Ajibade *et al*. (1979) have advocated dominantly ensialic mechanisms in the genesis of the schist belts, while Egbuniwe (1982) noted that some comprise oceanic elements with tholeiitic affinities. The rocks have been mapped, and information of such has been published. Three of the well-known schist belts are inside the study area (Maru, Anka and Zuru), with other rocks representing roughly twenty-six (26) different rock types in the study location (Figure 1).

MATERIAL AND METHODS

Source of the Data Used

The Nigerian Geological Survey Agency (NGSA) in Abuja provided eight airborne magnetic data sets for the study area: 50, 51, 52, 53, 73, 74, 75, and 76, which were merged to give the total magnetic intensity data export as the TMI map of the study area (Figure 2). The survey was carried out from 2005 to 2009, funded by the Nigerian Federal Government and the World Bank. The survey was conducted in two phases.

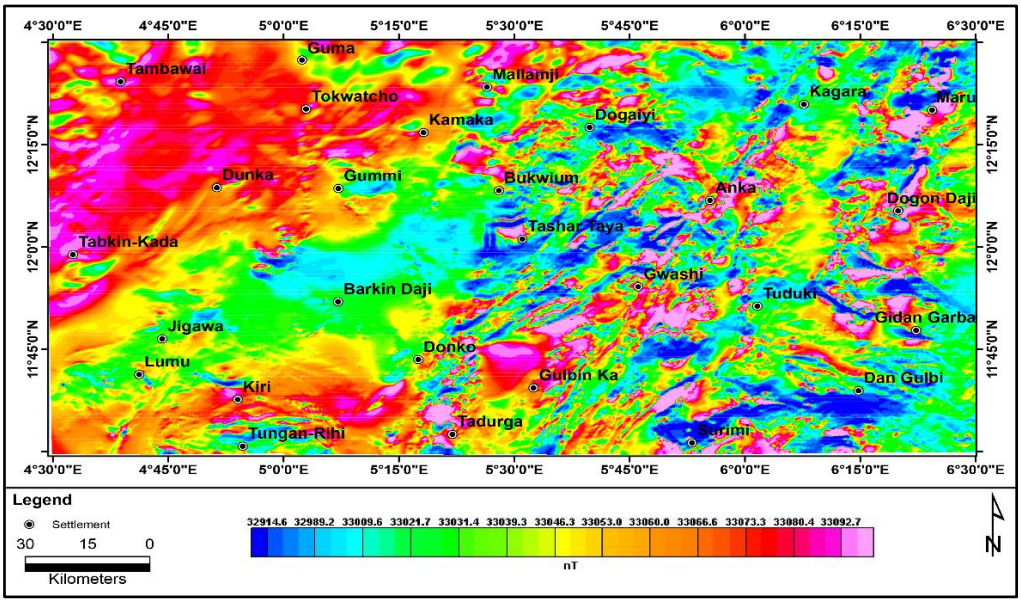

Figure 2: Total Magnetic Intensity Map

The Nigerian government completely financed the initial phase, in which Fugro Aerial Surveys conducted all aerial geophysical data gathering, processing, and interpretation (Reford *et al.*, 2010). Phase 1 included 826,000-line kilometers of magnetic and radiometric surveys, together with 24,000-line kilometers of time-domain electromagnetic surveys. Phase 2, finalized in August 2009, and encompassed 1,104,000-line kilometers of surveys, facilitated by the World Bank, with data collection and compilation overseen by Fugro Airborne Surveys.

Methodology

The total magnetic anomaly data (Figure 2) was subjected to regional and residual magnetic anomaly separation using upward continuation (Telford *et al*. 1990). We employed the upward continuation method because the method is subjective, and the magnetic data can be upward continued to any desired height of choice to get the residual magnetic data (Figure 3).

The reduced-to-pole (RTP) filter was applied to the residual magnetic anomaly data of the study area to position the anomalies above their causative sources (Li, 2008; Luo *et al*. 2010), using stable reduction to the pole with inclination of 1.49º and declination of -1.62º to get the RTP data (Figure 4). After that, we compute the analytic signal (AS) of the TMA (Roest *et al*. 1992), the computation of first vertical derivative and the computation of the 3D Euler deconvolution of RTP data (Reid *et al*. 1990).

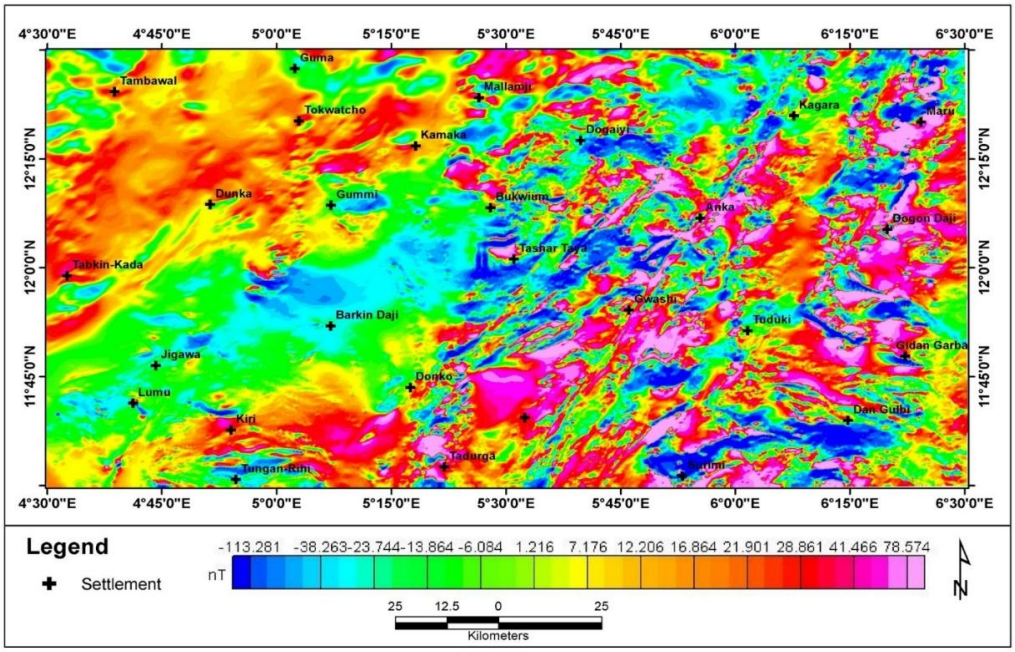

Figure 3: Residual Map of the Area

To locate structures and porphyry systems associated with mineral occurrences within the study area, the CET Porphyry Analysis was applied using its four extensions (plug-ins) that include Circular Feature Transform, Central Peak Detection, Amplitude Contrast Transform and Boundary Tracing (Holden *et al*. 2011; Core *et al*. 2009). The CET structures were correlated with the FVD by overlaying them on the FVD map. The analytic signal map, the porphyry system and the analytic signal were also correlated by overlaying them on each other.

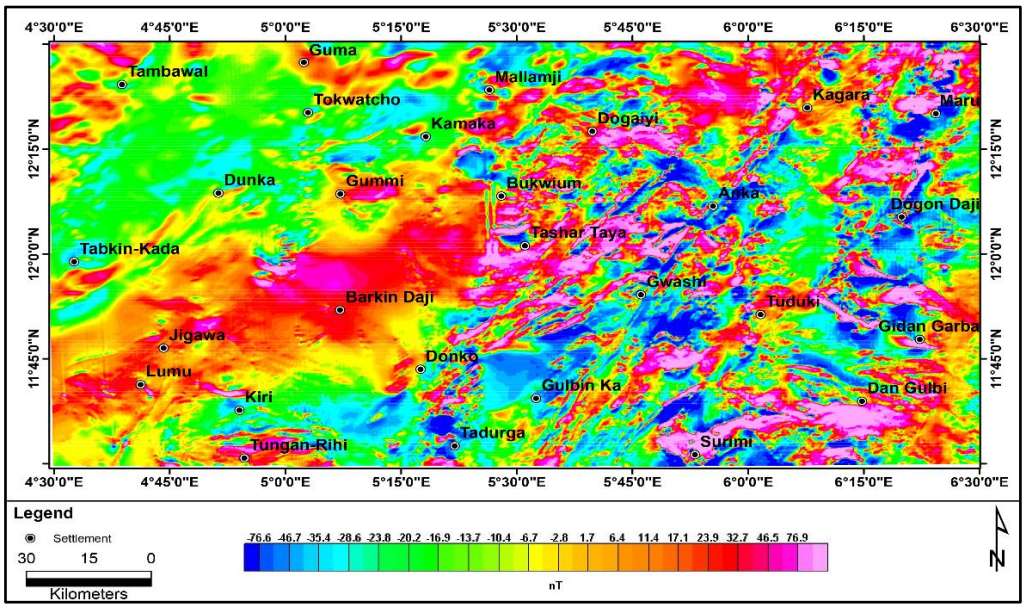

Figure 4: RTP Map of the Area

The basement topography beneath the sedimentary rocks of parts of the Sokoto basin was mapped using 2D geophysical modelling. Profiles L1-L1' to L3-L3' guided using the analytic signal map were drawn on the residual and digital elevation maps and were imported into the GM-SYS interface in the Oasis Montaj version 8.3 environment. Residual

magnetic and DEM (digital elevation map) data were integrated to construct a two-dimensional model aimed at improving understanding of the subsurface basement topography beneath the sedimentary basin. GM-SYS is an interactive, graphically based modelling software developed for the interpretation of magnetic and gravity datasets. A forward modelling technique was employed to achieve the closest possible match between the calculated response and the observed data.

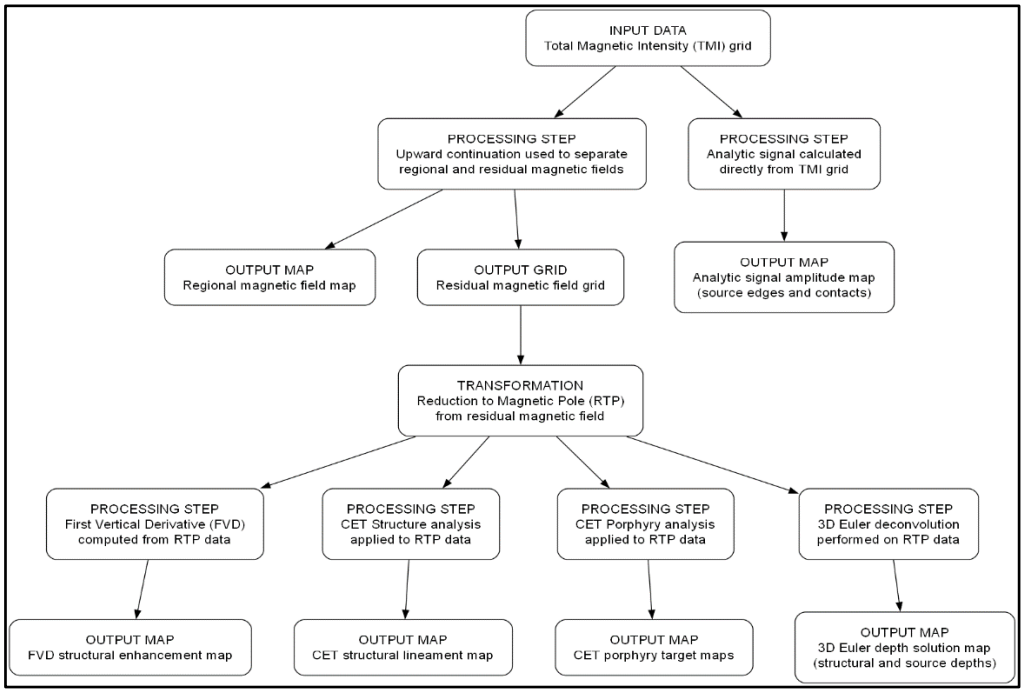

Figure 5: Flowchart of the methodology used in this work

This approach converts variations observed in potential-field data from residual magnetic anomalies into a representative subsurface geological model. The calculated response is iteratively compared with the observed anomaly, and model parameters are adjusted to enhance their agreement. This iterative cycle of geometry modification, anomaly computation, and comparison continues until a satisfactory correspondence is achieved between the calculated and observed anomalies, following the procedure described by Blakely (1995).

The Flowchart diagram for the methodology is as shown in (Figure 5), and the summary of the filtering techniques applied is in Table 1.

Table 1: Filtering techniques and their application

S/n	Technique	Equation	Application	Reference
1	Upward continuation	$F(x,y,-h) = \frac{h}{2\pi}\iint \frac{F(x,y,0)\,\partial x\,\partial y}{\sqrt{(x-x^i)^2+(y-y^i)^2+h^2}}$	Regional and residual separation	Telford *et al.*, 1990)
2	Reduction to pole	$M_p(u,v) = \frac{M_c M_p(u,v)}{[\sin(I)+i\cos(I)\,\cos(D-\Theta)]^2}$	To centre the anomaly above its causative sources	Luo *et al.* (2010)

3	Analytic signal	$\lvert A(X,Y)\rvert = \sqrt{\left(\frac{\delta M}{\delta x}\right)^2 + \left(\frac{\delta M}{\delta y}\right)^2 + \left(\frac{\delta M}{\delta z}\right)^2}$	Boundary, source location and structure	Roest *et al.* (1992)
4	First vertical derivative	$\frac{1}{n}\left[(U^2 + V^2)^{\frac{1}{2}}\right]^n$	Structures (Fault) delineation	Foss, 2011
5	3D Euler deconvolution	$(x - x_0)\frac{\delta T}{\delta x} + (y - y_0)\frac{\delta T}{\delta y} + (z - z_0)\frac{\delta T}{\delta z} = N(B - T)$	Border and depth estimation	Reid *et al.* (1990), Thompson (1982)
6	CET grid analysis	It is used for magnetic structural analysis.	To reveal magnetic lineaments	Holden *et al.*, 2011; Core *et al.*, 2009
7	CET porphyry analysis	Applied for porphyry detection	To reveal intrusive porphyry centres	Holden *et al.*, 2011; Core *et al.*, 2009

RESULTS AND INTERPRETATIONS

Results

Analytic Signal (AS) Map

The AS map (Figure 6) has outlined all the edges and source locations within the study area, and this depends on the variation in the distribution of magnetic sources within the study area.

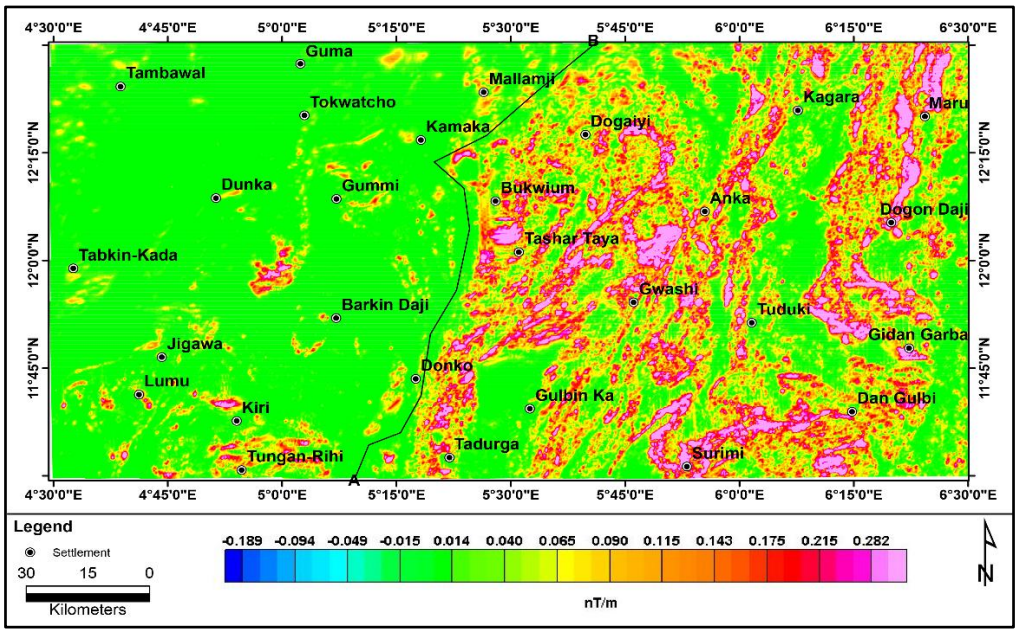

Figure 6: Analytic Signal Map of the Study Area

The AS map here also shows lithological contrasts (Figure 6), as the map has divided the study area into two parts. The right side of the map is specifically basement with high analytic signal amplitude, while the left parts highlight a portion of the Sokoto basin that is signified by very low amplitude (-0.015 nT/m).

The AS map demonstrates three distinct magnetic zones in this study area, determined by the amplitude of the anomalies present. Portions exhibiting low to medium analytic signal with amplitude ranges of -0.189 nT/m to 0.065 nT/m, medium magnetic zones (MM) with amplitudes from 0.065 nT/m to 0.143 nT/m, and areas characterised by high magnetic anomaly zones with amplitudes ranging from 0.143 nT/m to 0.282 nT/m are identified around Tadurga, Gwashi, Anka, Tunga Rahi Gidan Garba, Maru, Dan Gulbi, Mallaji, Danko, and Surimi. An isolated magnetic anomaly, typically round in shape and spanning several meters in the west-central portion of the map within the quartzite and quartz schist, may be indicative of magmatic intrusion (Figures 1 and 6). Those occurring within the central portion of the map and spanning toward the east end associated with the medium-grained biotite and hornblende granite, quartzite and quartz schist, biotite hornblende granodiorite, quartz diorite, slate phyllite meta-siltstone (locally hornfelsic), hypersthene quartz diorite, granite gneiss, migmatitic granite gneiss, muscovite schist and quartzite, and migmatite (Figures 1 and 6) might have arisen from accumulations of magnetite and/or pyrrhotite which may be associated with economic-grade mineral deposits. Such deposits precipitating from mineral-bearing solutions are frequently located within or adjacent to major faults. The high-amplitude areas could also represent areas of later tectonic activities where magma intruded into the preexisting rock skin and solidified in the fractures, faults, and joints left by earlier tectonic activities.

First Vertical Derivative (FVD) Map

The derivative filter is good in the amplification of faults/lineaments using potential field data (magnetic and gravity data), (Wang and Meng, 2019; Cooper, 2023; Sun *et al*., 2016; Ansari and Alamdar, 2011; Cooper and Cowan, 2011).

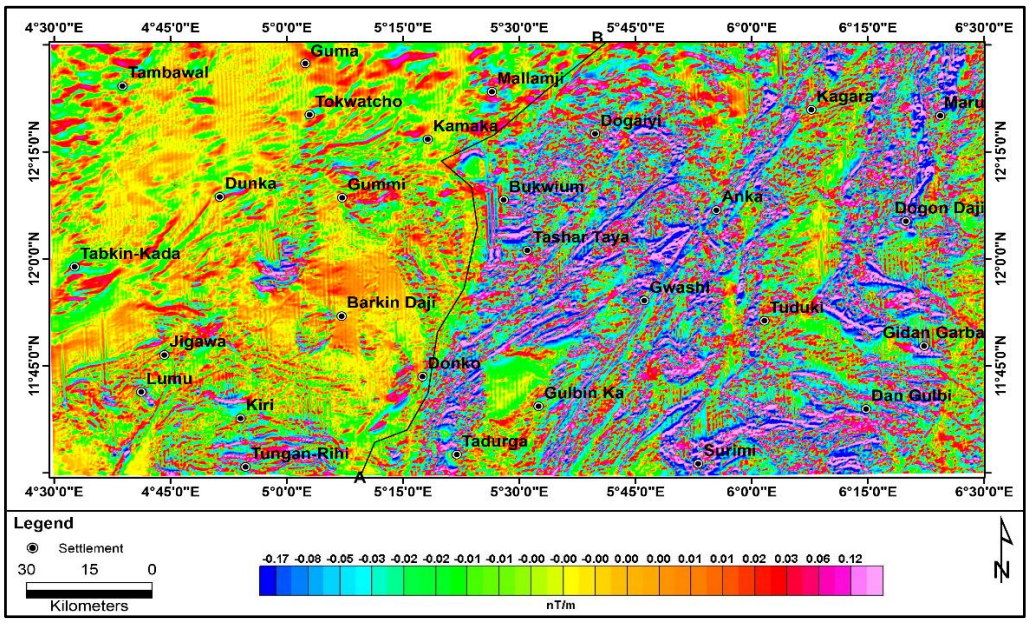

Figure 7: FVD map of the study area

The FVD map of the study area (Figure 7) has amplified the short wavelength anomalies within the centre of the map (around Bukwuim and Tashar Taya) toward the east (around Anka, Dogon Daji, Gwashi, Tuduki and Gidan Garba), indicating shallow depths

within the exposed basement region and also highlighting structures within this area. This is contrary to the western portion of the map with long wavelength signatures (around Barkin Daji, Gummi, Dunka, Gumi, Tambawal and Tabkin-Kada) within the sedimentary portion of the study area. Visual inspection of the anomaly trend has highlighted it to be Northeast to Southwest (NE-SW) orientated. Just like the AS map (Figure 6), with the FVD map, we have been able to clearly distinguish the sedimentary and basement portions of the study area. The basement to the right has a short wavelength, while the sedimentary portion to the left has a predominantly long wavelength. Comparing the AS map (Figure 6) to the FVD map (Figure 7), we can clearly see that the two maps correlate, as portions with high analytic signal amplitude on the AS map are portions of short wavelength on the FVD map with structures. Which also implies that the structures are pathways for emplacing gold and other minerals within the study area.

Application of CET Structural Plug-In

Figure 8 represent the CET structural map of the study area. Its highlights intense deformation and dense structural fabric in the central part of the study area, with similar trends extending eastward. These features are indicative of shallow basement settings and align with zones of high analytic signal amplitude (Figure 6) and short-wavelength anomalies on the first vertical derivative map (Figure 7). Structural trends as observed are WNW-ENE, NE-SW, NNE-SSW, and NW-SE directions. The structural density map of the delineated CET map (Figure 9) reveals five structural density zones within the study area. Very low structural density zones (0-0.133 km/km^2), low structural density zones (0.133-0.265 km/km^2), medium structural density zones (0.265-0.397 km/km^2), high structural density zones (0.397-0.529 km/km^2), and very high structural density zones (0.529-0.661 km/km^2).

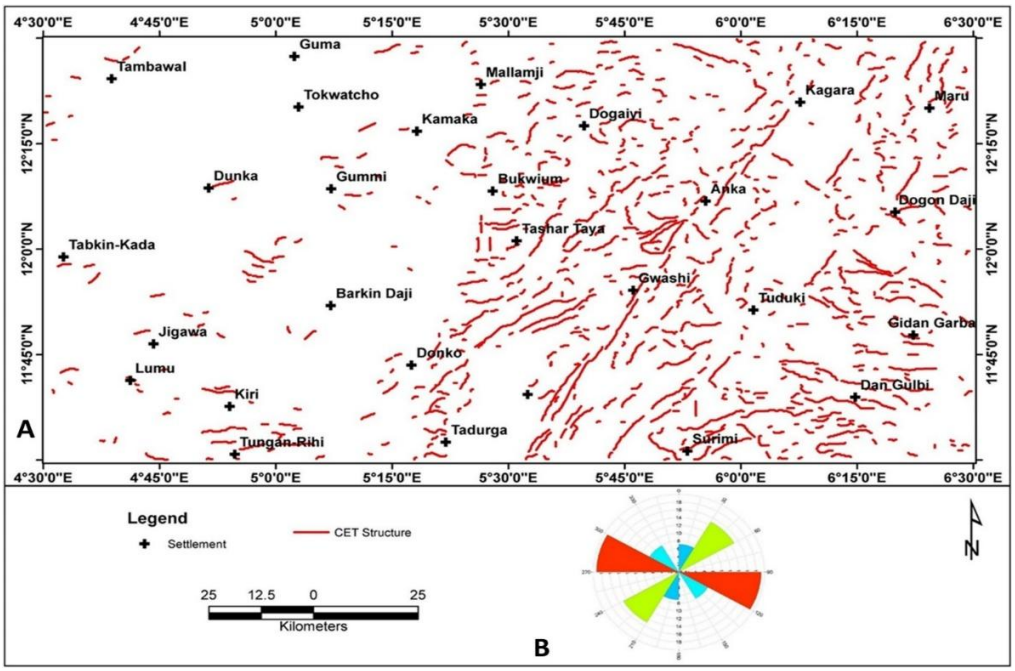

Figure 8: CET Structural Map of the Area

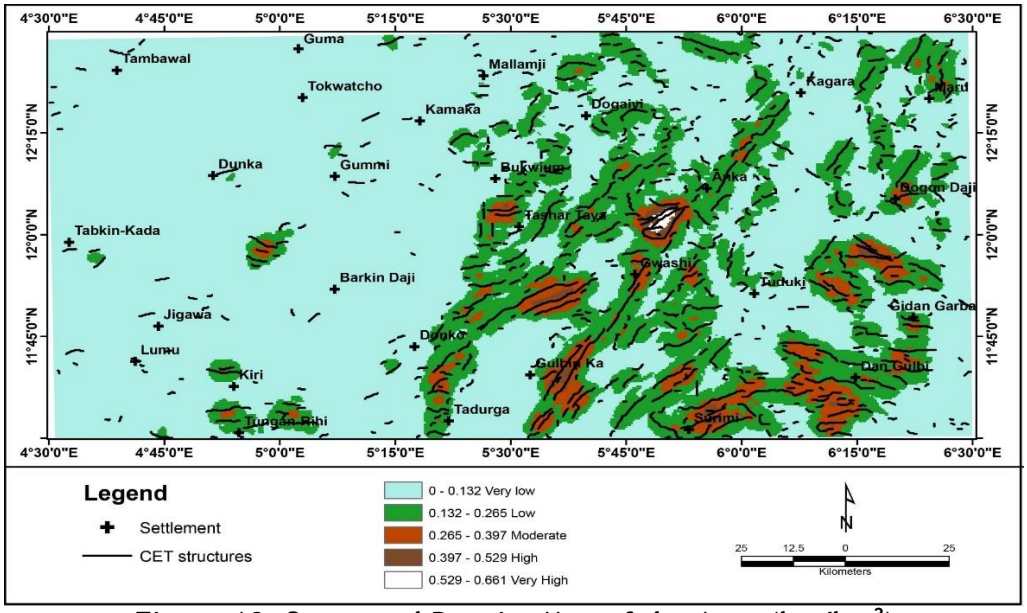

Figure 10: Structural Density Map of the Area (km/km^2)

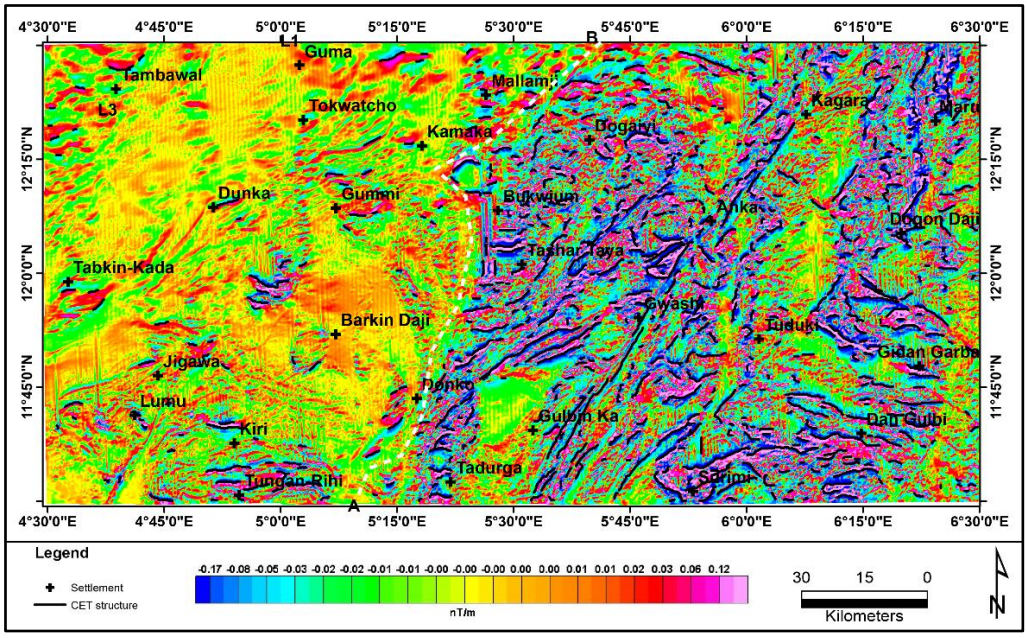

Figure 10: FVD map with CET Structures

The implication for the high and very high structural density is that these portions are portions of interest (for gold mineralization) as structures generally control movement of hydrothermal fluid and emplacement of ore minerals (Yin et al., 2025; Hronsky, 2020; Bedeaux et al., 2017; Tripp and Vearncombe, 2004; Tomlinson et al., 1988). The CET structures were overlaid on the FVD map (Figure 10), and the structures were observed to correlate with the FVD short wavelength signatures highlighting the structures within the study area.

Application of CET Porphyry Analysis Plug-In

Figure 11 represents the porphyry intrusions superimposed with CET structures within the study area. Porphyry mineralization exemplifies the magnetic characteristics associated

with alterations, as extensive areas of hydrothermal alteration typically exhibit distinct magnetic properties in contrast to unaltered geology (Tapia *et al.*, 2016; Riveros *et al.*, 2014).

These hydrothermal alterations have manifested in centralized, near-circular zones encircling a circular intrusive center (Figure 11) and aided in delineating anticipated porphyry systems linked to hydrothermal alteration within the study area. The predictions indicated by black circular to subcircular shapes on the CET porphyry analysis map, superimposed with CET structures (Figure 11), demonstrate that dike-like formations detected using the CET technique are structurally oriented along four principal trend lines. The structural trends are aligned WNW-ENE, NE-SW, NNE-SSW, and NW-SE.

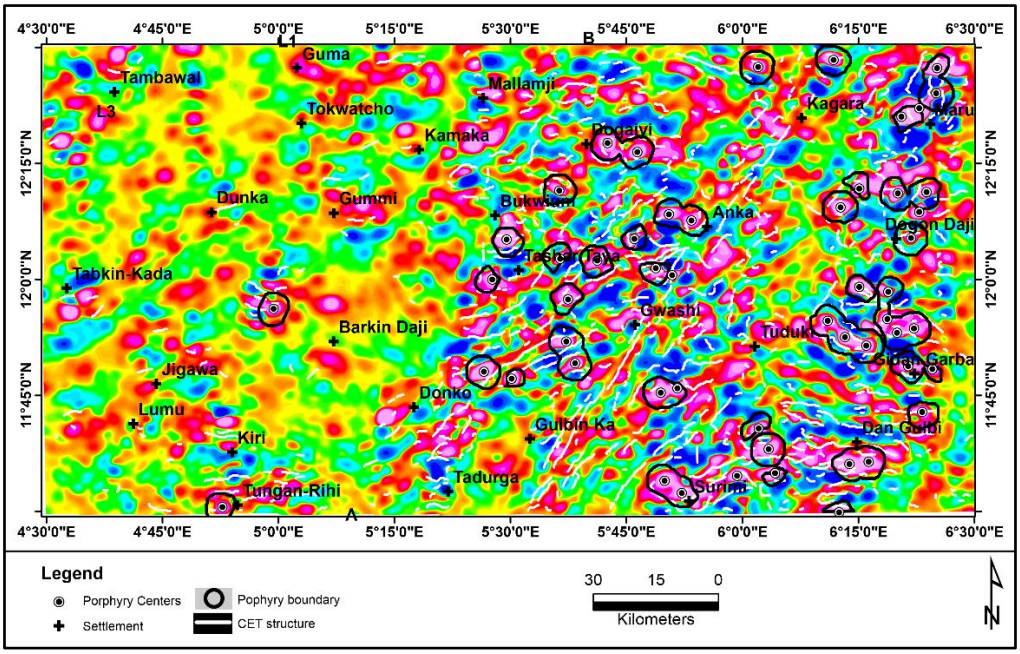

Figure 11: Porphyry intrusion with CET structure

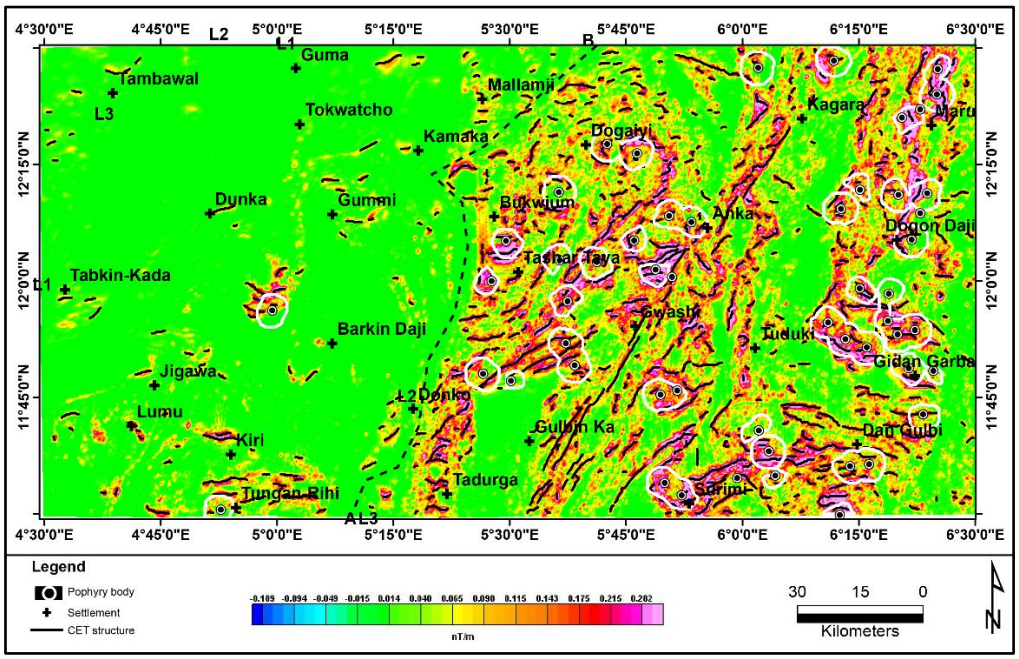

Figure 12: AS map overlay with CET structures and Porphyry bodies

The CET porphyry map exhibits a strong correlation with the analytic signal map (Figure 12), indicating areas with significant variations in magnetic intensities within the study area. This suggests that the structures present may contain various solid minerals, as these structures serve as conduits for mineralization fluids that permeate and deposit within the host rocks, including Gold, Pb-Zn mineralization and other undiscovered minerals that warrant further exploration. Previous research has confirmed the presence of gold alongside lead-zinc mineralization within the Nigerian schist belts, including the study area (Ogah and Abubakar, 2024; Akinlalu, 2023; Umaru *et al.*, 2022; Arogundade *et al.*, 2021; Augie *et al.*, 2022a; Sani *et al.*, 2019; Kudamya *et al.*, 2014; Obaje, 2009; NGSA, 2006).

3D Euler Deconvolution

Euler deconvolution is a popular depth and border estimator (Pasteka and Kusnirak, 2020; Ghosh *et al.*, 2012; Kuttikul *et al.*, 1995). Figure 13 illustrates the 3D Euler depth solutions with a structural index SI (N=1 for sill/dyke/fault) within the study area. These border and depth solutions are categorized into five groups: below 150 m, from 150 m to 300 m, from 300 m to 450 m, from 450 m to 600 m, and above 600 m. The Euler solutions in the basement portion of the study area aligns with the trends depicted in the CET structural map (Figure 8). Also, these Euler solutions are predominant within the northwestern portion of the study area with characteristics that are peculiar to the sedimentary basins > 450 m (Figure 15).

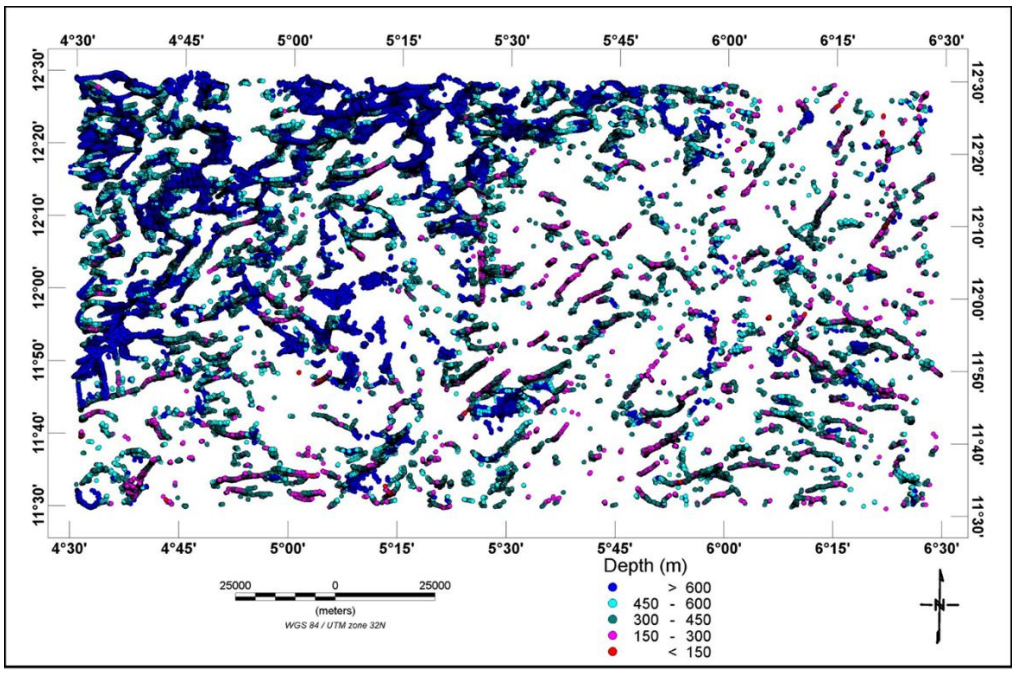

Figure 13: 3D Euler Deconvolution map of the area (SI =1)

Interpretation of the 2D Models

The analytic signal (AS) map (Figure 14) was used to delineate the contact between the basement and sedimentary units and also provided a basis for selecting profile lines within the sedimentary basin. The eastern portion of the map is dominated by the basement complex, whereas the western sector is largely occupied by the sedimentary basin. To investigate the basement topography beneath parts of the Sokoto Basin and its surroundings—features thought to be closely associated with mineralized structures in the

overlying sedimentary sequence—two-dimensional geophysical modelling was conducted. This modelling utilized magnetic data from profiles L1–L11 to L3–L31 extracted from the residual magnetic map (Figure 15), together with topographic information derived from the digital elevation model (Figure 16).

Profile L1-L1[1]

Figure 15 represents 2D section L1-L1[1] with NE-SW trend and stretching from NW of Tabkin-Kada to the NW of Guma in the northwestern part of the study area (Figures 14, 15 and 16).

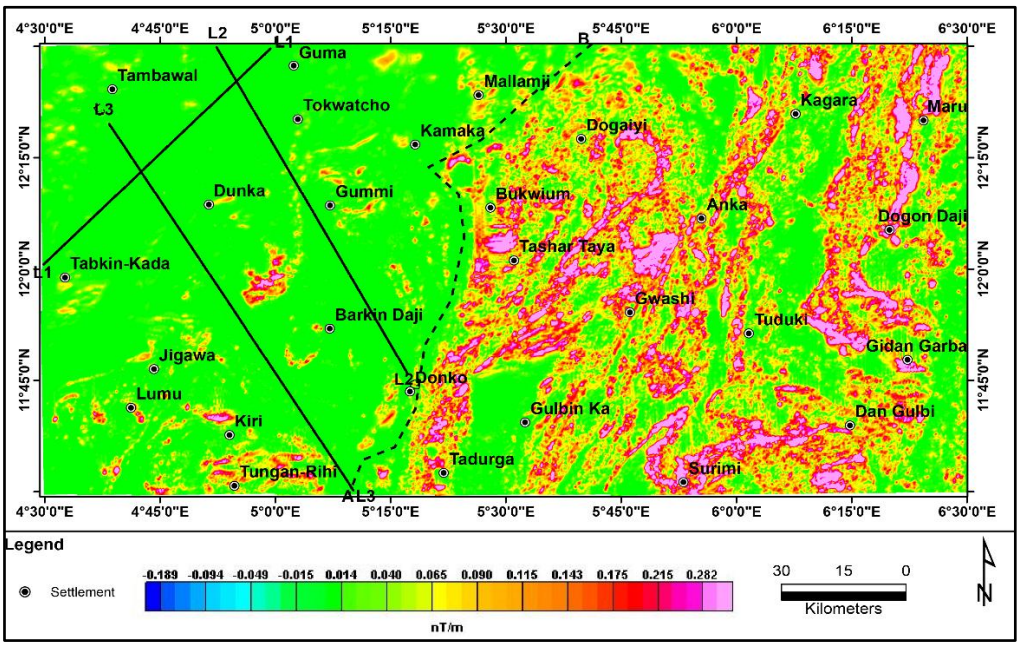

Figure 14: AS map with 2D profiles

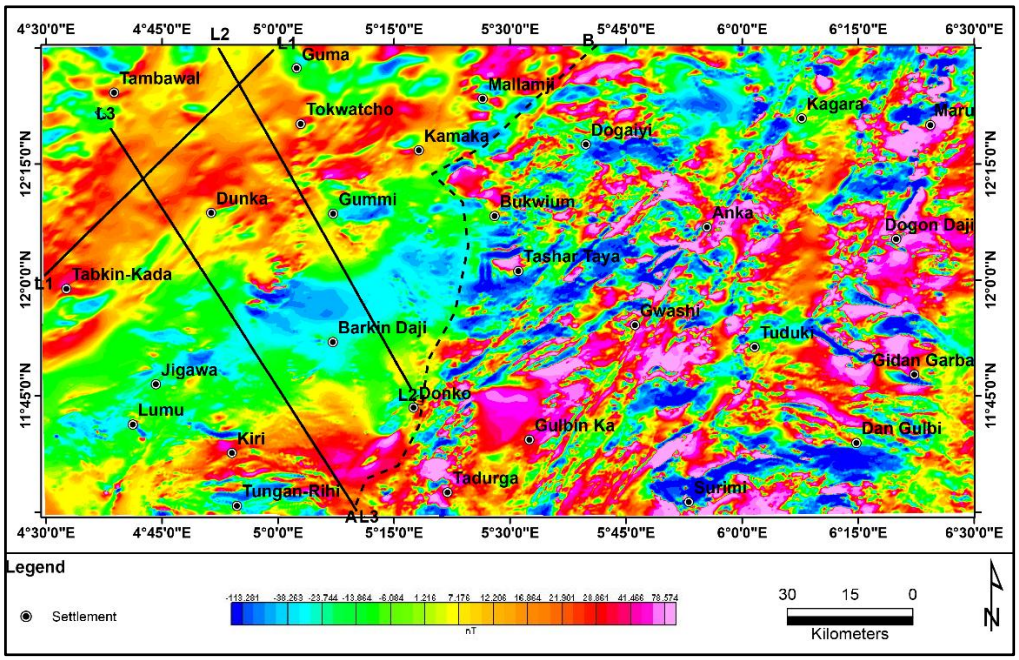

Figure 15: Residual magnetic intensity map with 2D profiles

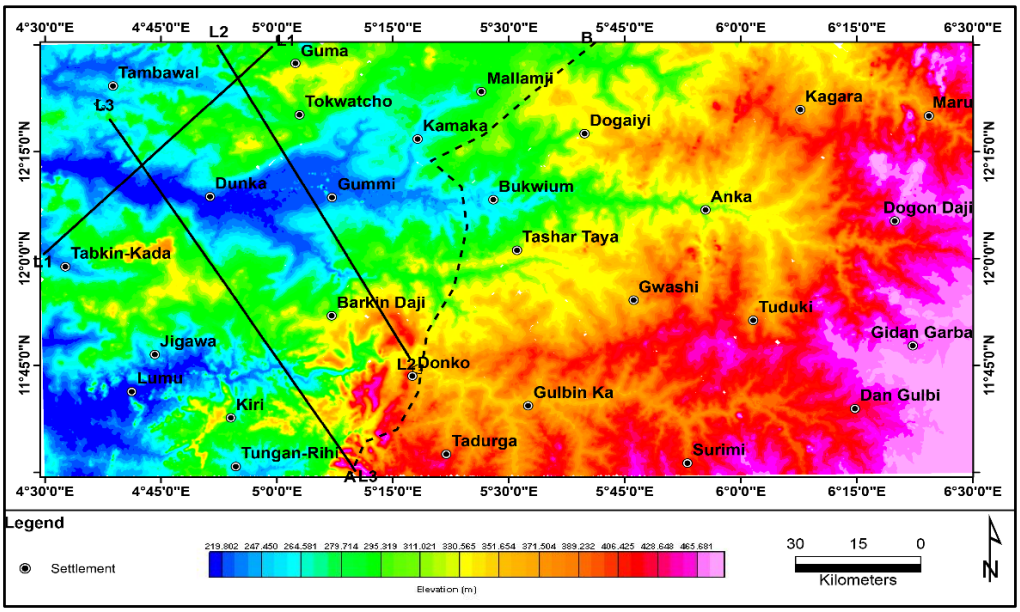

Figure 14: Digital elevation map with 2D profiles

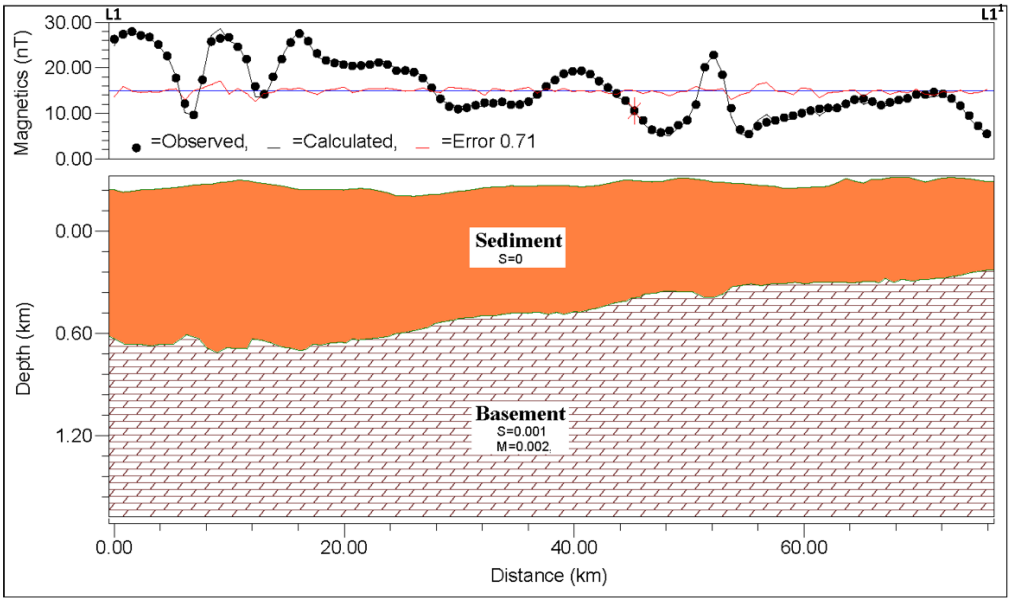

Figure 15: 2D profile L1-L1^1

The section along profile L1-L1^1 stretches about 0 to 72 km and reveals two primary layers. At the top, there's a non-magnetic sedimentary cover with a susceptibility of S = 0. Right beneath it, we find a magnetic crystalline basement with a susceptibility of S = 0.001 SI and a magnetization of M = 0.002. The sediments throughout this profile are about 0.55 to 0.7 km thick, indicating that the basement is relatively shallow.

As we move along the 72 km distance, the basement surface gently rises and falls, becoming a bit deeper toward the right, which suggests that the sediments are thickening as we approach the main Sokoto Basin. When it comes to mineral exploration along this 0-72 km profile, the model indicates that the schist belt basement, which is our main target, can be accessed with moderate drilling depths. Areas where the basement is closer to the surface and the sediment cover is thinner are top priority, as fractures and shear zones are likely to concentrate there, potentially hosting gold and base metal deposits. Meanwhile,

the deeper sections toward the basin's interior might favor strata bound mineralization near the base of the sediments at the contact with the basement.

Profile L2-L2^1

Figure 16 represents the 2D section of profile L2-L2^1 with NW-SE trend and passes between Tambalwal and Guma, Dunka and Tokwatcho, Gummi and Barkin Daji (Figures 14, 15 and 16). Profile L2-L2^{1}stretches roughly 0 to 94 km and runs in a NW-SE direction. Along with this profile, the sediments are thicker compared to the previous profile (profile L1-L1^1), with the basement lying mostly between 0.8 and 1.1 kilometers deep, creating a broad, gentle dip in the center of the profile. This hints at a small sub-basin nestled within the Sokoto Basin margin. For those interested in mineral exploration, the shallow basement areas at end of the profile, where the sediment is thinner, are promising targets.

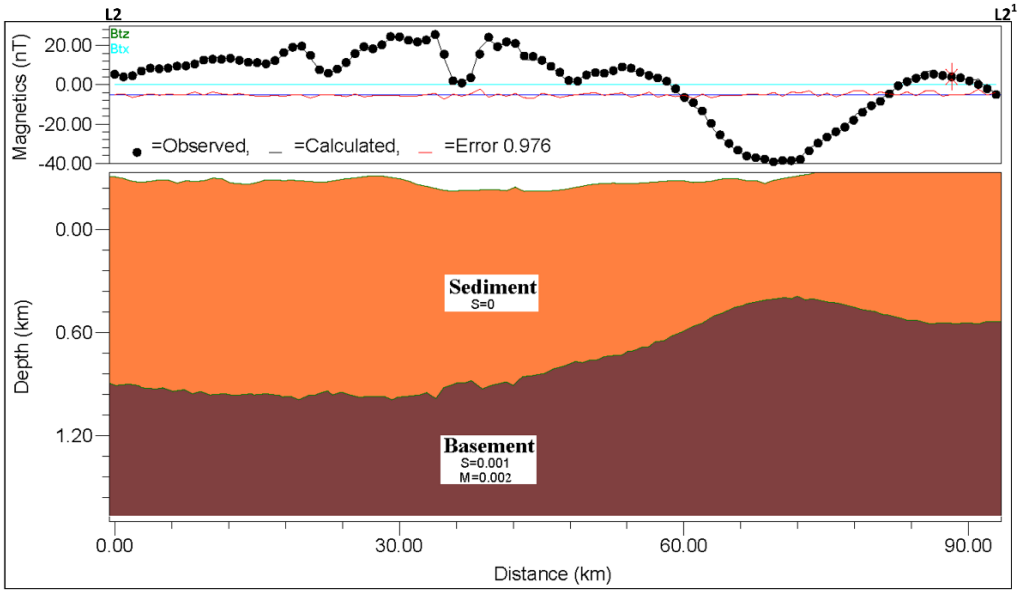

Figure 16: 2D profile L2-L2^1

This is because fractures and shear zones in the schist belt basement can be accessed with moderate drilling and might contain valuable mineralization.

Profile L3-L3^1

Figure 17 represents the 2D section of profile L3-L3^1 also trending in the NW-SE direction passing in between Tabkin-Kada and Dunka, Jigawa and Barkin Daji, Kiri and Donko, Tungan-Rihi and Tadurga(Figures 14, 15 and 16). The Profile L3-L3^1 stretches approximately from 0 to 110 km. In this area, the basement creates a broad uplift right in the center, sitting at about 1 km deep, while it gradually deepens towards both ends, reaching depths of around 0.8 to 1.2 km. This means that sediment is thinnest above the central basement high and thickest at the edges. For exploration purposes, the central section of L3 is particularly significant because the shallow basement, covered by a thin layer, is easier to investigate. It could have present of structures that may host minerals of interest. In contrast, the deeper edges may be more conducive to mineralization near the bottom of the thicker sedimentary layers.

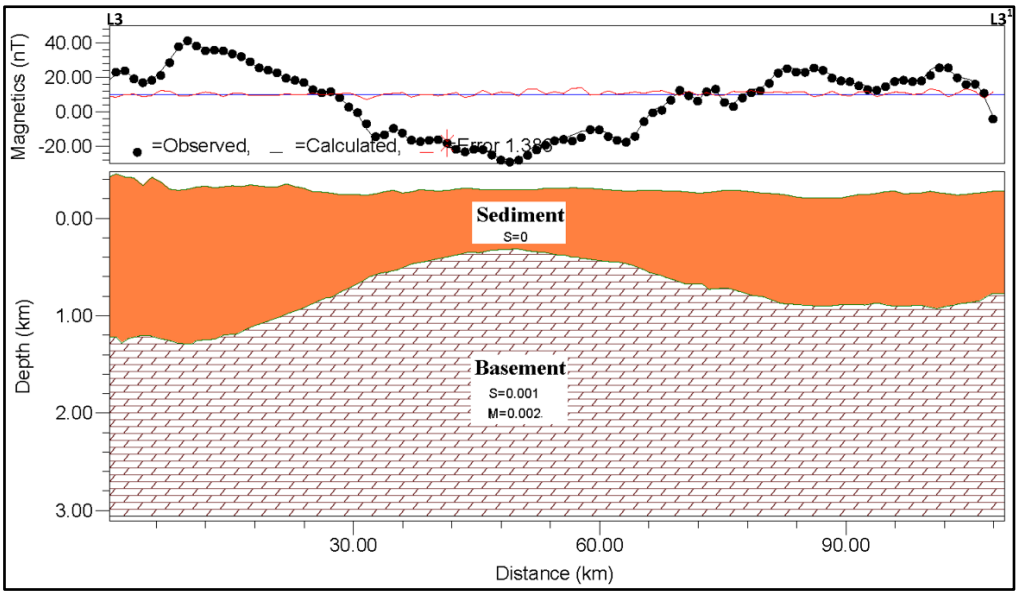

Figure 17: 2D profile L3-L3¹

Discussion

The integrated aeromagnetic interpretation has shed light on the structural framework and mineralization potential of the north-western Nigerian schist belts, as well as their transition into the Sokoto Basin. The AS map demarcates distinct magnetic boundary, showing low amplitudes over the western sedimentary portion and higher values over the eastern basement terrain. This disparity signifies the weak magnetization of the Cretaceous-Tertiary sediments compared to the crystalline schist-belt and granitoid rocks, providing a clear geophysical representation of the basin-basement boundary. Within the basement, areas of high analytic signal align with major lineament intersections and mapped granitoid and quartzite units, creating conditions that are favorable for both orogenic and porphyry-style systems.

The first vertical derivative enhances short-wavelength anomalies and uncovers a dense network of faults and fractures, particularly in the central and eastern regions. These structures follow WNW-ENE, NE-SW, NNE-SSW, and NW-SE trends, which correspond with the regional Pan-African fabrics previously identified in the Maru, Anka, and Zuru belts. Their alignment reinforces the idea that they serve as long-lasting conduits for hydrothermal fluids. Long-wavelength anomaly in the western section of the study area correlates with the presence of thick and more uniform sediments in the Sokoto Basin, along with lack of shallow magnetic sources in that area.

CET structural analysis and structural-density mapping provide a detailed look at how intense the deformation is. Areas with high and very high structural density are typically where several fault sets come together and where the amplitudes of analytic signals are notably high. These regions are seen as highly fractured blocks that have played a role in channeling and trapping mineralizing fluids. The strong correlation between these structural-density highs, elevated analytic signals, suggests that these areas are excellent candidates for further exploration of orogenic gold and related polymetallic mineralization.

The CET porphyry analysis sheds new light on potential intrusive centers that previous regional studies may have overlooked. Circular to subcircular magnetic features, which are thought to represent porphyry intrusions or magnetite-rich alteration cores, tend to cluster along major structural trends and at their intersections. Their overlap with high analytic signal zones indicates that there may be magnetite addition or destruction linked to hydrothermal alteration. This pattern aligns with what we see in porphyry-style systems, where central intrusive stocks are surrounded by concentric alteration halos. The alignment of these centers with structures and high analytic signal amplitudes suggest that both orogenic shear zones and porphyry-related hydrothermal systems play a role in the mineralization of the region.

Euler deconvolution adds a valuable layer to our understanding of the structure by giving us depth estimates for magnetic sources. We find that depth solutions less than 300-450 meters are mostly located in the basement area and along the edges of the basin. This suggests that many of the faults, dykes, and porphyry centers we've identified are within reach for mining. On the other hand, deeper solutions that go beyond 450-600 meters are primarily found beneath the sedimentary cover, likely indicating the deeper basin fill and hidden basement highs.

The 2D GM-SYS models along profiles L1-L3 help to clarify this basement structure. Profile L1-L1[1] reveals a shallow basement at depths of about 0.55-0.7 kilometers, with smooth undulations near the basin margin. Profile L2-L2[1] shows a wide depression with basement depths ranging from 0.8 to 1.1 kilometers, which might indicate a local sub-basin. Meanwhile, profile L3-L3[1] features a central basement high with deeper edges on either side. These differences in basement relief are crucial for studies related to minerals and groundwater. The combination of analytic signals, derivative filters, CET plug-ins, Euler depths, and 2D modeling has created a clear understanding of the structural factors influencing mineralization. This study shows that when aeromagnetic data is analyzed using modern structural and porphyry analysis tools, it can elevate regional exploration in northwestern Nigeria from merely mapping gold-bearing shear zones to a much deeper evaluation of porphyry-style systems and basin-margin target.

CONCLUSION

The aeromagnetic study conducted in parts of northwestern Nigeria has revealed that the area is defined by a well-structured basement complex that transitions westward into the sedimentary layers of the Sokoto Basin. The analytic signal and first vertical derivative maps effectively distinguish the magnetic basement from the less magnetic sediments, uncovering a network of faults and fractures that primarily trend WNW-ENE, NE-SW, NNE-SSW, and NW-SE. Through CET structural and structural-density analysis, we can identify zones of significant deformation that could align with gold deposits and areas of high analytic signal. These zones are seen as the main pathways and traps for hydrothermal fluids.

CET porphyry analysis brings to light several circulars to subcircular magnetic centers that are closely associated with major structures and high analytic signal amplitudes. These centers are interpreted as intrusive bodies along with their alteration zones, which could potentially host porphyry-style mineralization. Euler depth solutions and 2D modeling across three profiles along the basin margin suggest a sediment thickness ranging from about 0.55 to 1.2 km, along with a gently undulating crystalline basement featuring local highs and

lows. Collectively, these findings indicate a promising potential for structurally controlled gold and Pb-Zn deposits within the schist belt basement and along the margins of the Sokoto Basin, providing a solid geophysical foundation for more in-depth follow-up studies.

REFERENCES

Abaa, S. I. (1983). The structure and petrography of alkaline rocks of the Mada Younger Granite Complex, Nigeria. Journal of African Earth Sciences, 3, 107–113.

Adebayo, A. E., Abolarinwa, D. D., and Omohimoria, C. U. (2025). Geological Mapping and Petrostructural Characterization of Precambrian Rocks in Oke-Ode Area, Southwestern Nigeria: Implications for Regional Tectonics and Geological Evolution. International Journal of Science and Research Archive, 16(2), 332–342. https://doi.org/10.30574/ijsra.2025.16.2.2329

Adejuwon, B. B. Okiyi, I. M. and Shuaibu A.M (2025) application of geophysical techniques for gold exploration in northcentral Nigeria. Geological Behavior (GBR) DOI: http://doi.org/10.26480/gbr.01.2025.01.10

Akinlalu, A. A. (2023). Radiometric mapping for the identification of hydrothermally altered zones related to gold mineralization in Ife–Ilesa Schist Belt, Southwestern Nigeria. Indonesian Journal of Earth Sciences, 3(1), 51.

Alabi, O. O., Sedara, S. O., Olatona, G. I., Olaleye, A. O., and Kasali, A. A. (2025). Mineral Resource Exploration Potential in the Ado-Ekiti-Ilesa Region of Southwest, Nigeria using Aeromagnetic Survey. Deleted Journal, 34(3), 43–52. https://doi.org/10.62292/10.62292/njp.v34i3.2025.400

Ajibade, A. C., Fitches, W. R., and Wright, J. B. (1979). The Zungeru mylonites, Nigeria: recognition of a major unit. Revue de Geologie et de Geographie Physique, 21, 359–363.

Aliyu, S.B., Adetona, A.A., Rafiu, A.A., Ejepu, J.S. and Adewumi, T. (2021). Delineating and Interpreting the Gold Veins Within Bida and Zungeru Area, Niger State Nigeria, Using Aeromagnetic and Radiometric Data. Pakistan Journal of Geology (PJG) 2021, Vol.5, Issue 2, pp 41-50.

Ansari, A. H., and Alamdar, K. (2011). An improved method for geological boundary detection of potential field anomalies. Journal of Mining and Environment. https://doi.org/10.22044/JME.2011.13

Arogundade, A. B., Awoyemi, M. O., Ajama, O. D., Falade, S. C., Hammed, O. S., Dasho, O. A., and Adenik, C. A. (2021). Integrated aeromagnetic and airborne radiometric data for mapping potential areas of mineralisation deposits in parts of Zamfara, Northwest Nigeria. Pure and Applied Geophysics. https://doi.org/10.1007/s00024-021-02913-w

Augie, A. I., Salako, K. A., Rafiu, A. A., and Jimoh. M. O. (2022a). Geophysical assessment for gold mineralization potential over the southern part of Kebbi State using aeromagnetic data. Geology, Geophysics and Environment, 48(2), 177–193.

Augie, A. I., Adamu, A., Salako, K. A., Alkali, A. G., Narimi, A. M., Yahaya, M. N., and Sani, A. A. (2022). Assesment for gold mineralisation potential over anka schist belts nw nigeria, using aeromagnetic data. FUDMA JOURNAL OF SCIENCES, 5(4), 235–242. https://doi.org/10.33003/fjs-2021-0504-810

Augie, A. I., Salako, K. A., Rafiu, A. A., and Jimoh, M. O. (2022). Geophysical assessment for gold mineralization potential over the southern part of Kebbi State using aeromagnetic data. Geology, Geophysics and Environment, 48(2), 177–193. https://doi.org/10.7494/geol.2022.48.2.177

Augie, A. I., Salako, K. A., Rafiu, A. A., and Jimoh, M. O. (2024). Integrated Geophysical Investigation for Potential Gold Mineralised Zone within Lower Part of Zuru Schist Belts, NW Nigeria. Deleted Journal, 33(2), 1–14. https://doi.org/10.62292/njp.v33i2.2024.212

Bedeaux, P., Pilote, P., Daigneault, R., and Rafini, S. (2017). Synthesis of the structural evolution and associated gold mineralization of the Cadillac Fault, Abitibi, Canada. Ore Geology Reviews, 82(82), 49–69. https://doi.org/10.1016/J.OREGEOREV.2016.11.029

Blakely, R. J. and Simpson, R. W. (1995). Approximating edge of source bodies from magnetic or gravity anomalies. Geophysics, 51, 1494-1498.

Chang, C., Xiao, K., Luo, G., and Sun, L. (2024). Influence of different tectonic settings on fracture formation and fluid flow around upper-crustal magmatic intrusion: insights from numerical modelling. Earth Science Informatics. https://doi.org/10.1007/s12145-024-01255-0

Chen, Y., Wang, Y., Wang, J., Li, D., Geng, J., Luo, J., and Wang, R. (2025). The Fluid Evolution and Metallogenic Processes of the Liba Gold Deposit, West Qinling, China: Insights from the Texture, Trace Elements, and H-O Isotope Geochemistry of Quartz. Minerals, 15(9), 956. https://doi.org/10.3390/min15090956

Cooper, G. R. J., and Cowan, D. (2011). A generalized derivative operator for potential field data. Geophysical Prospecting, 59(1), 188–194. https://doi.org/10.1111/J.1365-2478.2010.00901.X

Cooper, G. R. J. (2023). Novel Second-Order Derivative-Based Filters for Edge and Ridge/Valley Detection in Geophysical Data. Minerals. https://doi.org/10.3390/min13091229

Core, D., Buckingham, A., and Belfield, S. (2009). Detailed structural analysis of magnetic data done quickly and objectively. Specialist group in economic geology (SGEG) Newsletter. (April).

Dou, Z., Zhou, Z., Wang, J., and Huang, Y. (2024). Concepts, Structure, and Properties of Fractured Media (pp. 19-41). https://doi.org/10.1007/978-981-99-9187-7_2

Egbuniwe, I. G. (1982). Geotectonic evolution of the Maru Belt, NW Nigeria (Unpublished doctoral dissertation). University of Wales, Aberystwyth.

Emumejaye, K., Okpara, E. C., Olaoye, M. A., Ishola, S. A., Biere, P. E., Mustapha, O., Banks, C. E., Onwudiwe, D. C., Makinde, V., and Gbadebo, A. M. (2025). A health risk assessment of the heavy metal levels in soil from Itagunmodi and Iperindo mining belt, Southwest Nigeria. Discover Environment, 3(1). https://doi.org/10.1007/s44274-025-00326-3

Fedi, M., (2002): Multiscale derivative analysis: a new tool to enhance detection of gravity source boundaries at various scales. Geophysical Research Letters 29 (2). 1029 (16-1- 16-4).

Foss, c. (2011). Magnetic data enhancement and depth estimation. (H. Gupta, Ed.) Encyclopedia of Earth Sciences Series, 735-746

Gadge, P. P., Bhajantri, M. R., and Kapur, K. (2023). Optimization of Hydraulic Design of Spillways and Its Appurtenant Structures-Role of Physical Model Studies (pp. 341–352). Springer Nature. https://doi.org/10.1007/978-981-99-1890-4_27

Gaafar, I. M. (2012). Geophysical signature of the vein-type uranium mineralisation of Wadi Eishimbai, Southern Eastern Desert, Egypt. Arabian Journal of Geoscience, 5, 1185-119

Gaafar, I. M. (2014). Geophysical mapping, geochemical evidence, and mineralogy for Nuweibi rare metal albite granite, Eastern Desert, Egyptian. Open Journal of Geology, 4, 108–136.

Gaafar, I. (2015). Integration of geophysical and geological data for delimitation of mineralized zones in Um Naggat area, Central Eastern Desert, Egypt. NRIAG Journal of Astronomy and Geophysics, 4, 86-99.

Ganiyu, S. A., Olutoki, J. O., Ajewole, O. O., and Bello, A. (2025). Characterization and Monitoring of Leachate Plume migration in Active Dumpsite within Basement Complex of Southwest Nigeria using Integrated Geophysical Methods. Deleted Journal, 34(3), 174–188. https://doi.org/10.62292/10.62292/njp.v34i3.2025.441

Ge, T., Qiu, L., He, J., Fan, Z., Huang, X., and Xiong, S. (2020). Aeromagnetic identification and modeling of mafic-ultramafic complexes in the Huangshan-Turaergen Ni-Cu metallogenic belt in NW China: Magmatic and metallogenic implications. Ore Geology Reviews, 127. https://doi.org/10.1016/j.oregeorev.2020.103849

Ghosh, G. K., Khanna, A. K., and Singh, S. N. (2012). Application of Euler Deconvolution of Gravity and Magnetic Data for Basement Depth Estimation in Mizoram Area. https://doi.org/10.3997/2214-4609.20143715

Grant, F. S. (1978). Review of data processing and interpretation methods in gravity and magnetics, 64-71, Geophysics, (37); 647-661

Guillou-Frottier, L., Milesi, G., Roche, V., Duwiquet, H., and Taillefer, A. (2023). Heat flow, thermal anomalies, tectonic regimes and high-temperature geothermal systems in fault zones. Comptes Rendus Geoscience, 356(S2), 1-33. https://doi.org/10.5802/crgeos.213

Guo, H., Mao, X., and Huang, J. (2024). 3D Prospectivity Modeling of the Nibao Carlin-Type Gold Deposit, China: Insights into Mineralization Localization and Gold Exploration. https://doi.org/10.20944/preprints202404.1143.v1

Han, R., Wu, J., Zhang, Y., Chen, Q., and Sun, B. (2024). Oblique distribution patterns and the underlying mechanical model of orebody groups controlled by structures at different scales. Dental Science Reports, 14. https://doi.org/10.1038/s41598-024-55473-z

Heincke, B., Szwillus, W., Freienstein, J., Ebbing, J., Gaina, C., Ruppel, A., Dilixiati, Y., and Wansing, A. (2025). A new magnetic anomaly map for Greenland based on a combination of equivalent source modeling and spherical harmonic expansion. https://doi.org/10.5194/essd-2025-448

Holden,E.J., Fu, S.C., Kovesi,P., Dentith, M., Bourne, B., Hope, M., (2011): Automatic identification of responses from porphyry intrusive systems within magnetic data using image analysis. Journal of Applied Geophysics 74 (2011) 255–262.

Hronsky, J. (2020). Deposit-scale structural controls on orogenic gold deposits: an integrated, physical process–based hypothesis and practical targeting implications. Mineralium Deposita, 55(2), 197–216. https://doi.org/10.1007/S00126-019-00918-Z

Idriss, A. A. (2025). Geology and Petrography of Kanawa Member of Pindiga Formation Exposed at Ashaka Cement Quarry of the Upper Benue Trough, Northeasten Nigeria. International Journal for Research in Applied Science and Engineering Technology. https://doi.org/10.22214/ijraset.2025.74248

Kang, R., and Guan, Q. (2025). High-resolution near-seafloor magnetic data processing and interpretation of hydrothermal activity on the arctic Gakkel ridge. 11. https://doi.org/10.1117/12.3084153

Kossov, G. A., Abashkin, V. V., Egorov, S. V., Makienko, D. O., and Gaeva, V. A. (2025). A new state-of-the-art technique for textural and structural microimager data analysis using deep learning algorithms. Георесурсы, 27(3), 209–220. https://doi.org/10.18599/grs.2025.3.22

Kudamnya, E. A., Andongma, W. T., and Osumeje, J. O. (2014). Hydrothermal mapping of Maru schist belt, north-western Nigeria using remote sensing technique. International Journal of Civil Engineering (IJCE), 3(1), 59-66.

Kuttikul, P., Barritt, S., and Hanssen, R. (1995). Maximization of Geological Information in 3D Euler Deconvolution. https://doi.org/10.3997/2214-4609.201409312

Lawal, T. O., Sunday, J., Fawale, korede, Salami, M., and Adewumi, T. (2021). Use of Magnetic anomaly data to delineate subsurface structures and depth characterization of Lafiagi and its environs, Northcentral Nigeria. NRIAG Journal of Astronomy and Geophysics, 10(1), 155–167. https://doi.org/10.1080/20909977.2021.1900526

Li, X. (2008). Magnetic reduction-to-the-pole at low latitudes. Observations and considerations. The Leading Edge, 27(8), 961-1080. https://doi.org/10.1190/1.2967550

Li, S., Zhang, H., and Hou, Z. (2025). Mineralization at Different Structural Levels in the Crust. Acta Geologica Sinica-English Edition, 99(4), 1042–1058. https://doi.org/10.1111/1755-6724.15319

Li, J., Yamazaki, T., Sato, M., and Kuroda, J. (2025). Magnetic Mineral Assemblages of Diagenetically Reduced Sediments and Their Contributions to Paleomagnetic Signals. Journal Of Geophysical Research: Solid Earth, 130(10). https://doi.org/10.1029/2025jb032348

Liu, G., Yao, K., Niu, F., Li, J., Gao, J., Rong, J., Fu, Z., Zhang, W., Wang, Y., Zeng, J., Shi, W., Hu, J., Zhang, Z., Liu, J., and Liu, Z. (2024). Deep investigation of muography in discovering geological structures in mineral exploration: a case study of Zaozigou gold mine. Geophysical Journal International. https://doi.org/10.1093/gji/ggae057

Luo, Y., Xue. D. J., and Wang, M. (2010). Reduction to the pole at the geomagnetic equator. Chinese Journal of Geophysics 53(6) 1082-1089

Maarifa, E. J., Kariuki, P. C., and Mshiu, E. E. (2024). Mapping of surface hydrothermal mineral alterations and geological structures related to geothermal systems in the Songwe region, SW Tanzania. Geosystem Engineering. https://doi.org/10.1080/12269328.2023.2299481

Manekator, G. T., and Aigbedion, I. (2025). Assessment of gold mineralization potential using aeromagnetic and Aeroradiometric data in Dagbala Edo North, Nigeria. International Journal of Science and Research Archive, 16(1), 2210–2221. https://doi.org/10.30574/ijsra.2025.16.1.0047

McCurry, P. (1976). The geology of the precambrian to lower Palaeozoic rocks of northern Nigeria. A review. In: Kogbe CA (ed) Geology of Nigeria. Lagos: Elizabethan Publishers, 15-39.

Mindiashvili, G., Bluashvili, D., Lipartia, T., Jafaridze, N., and Benashvili, K. (2025). Application of Machine Learning to Hydrothermal System Analysis: Geochemical Insights from the Bektakari–Bneli Khevi Ore Knot, Southern Georgia. Bulletin of the Mineral Research and Exploration, 178(178), 1-2. https://doi.org/10.19111/bulletinofmre.1768420

Narimi, A. M., Adewuyi, R. abdulwaheed, Ahmed, U., Nda, A. I., Abubakar, F., and Bagare, A. A. (2025). Evaluation of solid mineral potentials in north western parts of Nigeria using aero radiometric and geochemical data sets. https://doi.org/10.21203/rs.3.rs-7464005/v1

Nigerian Geological Survey Agency. NGSA. (2006). Geology and structural lineament map of Nigeria.

Obaje, N.G. (2009) Solid minerals and Nigeria's economic development: Resource potential, challenges and prospects. *Journal of mining and geology, 56(2), 213-228*

Ogah, J., and Abubakar, F. (2024). Solid mineral potential evaluation using integrated aeromagnetic and aeroradiometric datasets. Arewa Scientific Reports, 14:1637. https://doi.org/10.1038/s41598-024-52270-6

Oghonyon, R., and Nnurum, E. U. (2025). Quantitative Analysis of Aeromagnetic Data for Geophysical Interpretations of Bamenda Massif, Southeastern Nigeria. International Journal of Scientific and Research Publications, 15(7), 36-38. https://doi.org/10.29322/ijsrp.15.07.2025.p16306

Ohaegbuchu, H. E., Dinneya, O. C., Esomchi, N., Uzoma, Uzoaru, S. I., and Musa, Y. (2025). Unconstrained 3D Inversion of Airborne Magnetic Data for Mineral Targeting in the Southwestern Nigerian Basement Complex. Deleted Journal, 34(3), 135–153. https://doi.org/10.62292/10.62292/njp.v34i3.2025.425

Okpoli, C. C., Idakwo, S. O., Olaniyan, O., and Chidi, P. E. (2025). Geotectonics and Exploration of Gold Mineralization in the Kushaka-Kusheriki Schist Belt North-Central Nigeria. Indonesian Journal of Earth Sciences, 5(1), A1250. https://doi.org/10.52562/injoes.2025.1250

Olomo, K. O., Bayode, S., Alagbe, S. A., Olayanju, G. M., and Olaleye, O. K. (2022a). Aeromagnetic Mapping and Radioelement Influence on Mineralogical Composition of Mesothermal Gold Deposit in Part of Ilesha Schist Belt, Southwestern Nigeria. NRIAG Journal of Astronomy and Geophysics, 11(1), 177-192. DOI: 10.1080/20909977.2022.2057147

Pasteka, R. and Kusnirak, D. (2020). Role of Euler Deconvolution in Near Surface Gravity and Magnetic Applications (pp. 223–262). Springer, Cham. https://doi.org/10.1007/978-3-030-28909-6_9

Pan, Y., Ni, C., Fan, J., Yang, R., Han, X., and Huang, Y. (2023). Characterization of the genesis and spatial variability in tectonic fractures in the Gaosong ore field (South China). PLOS ONE, 18(11), e0292023. https://doi.org/10.1371/journal.pone.0292023

Reford, S. W., Misener, D. J., Ugalde, H. A., Gana, J. S., and Olaniyan, O. (2010). Nigeria's nationwide high-resolution airborne geophysical surveys, conference. Society of Exploration Geophysicists (SEG) Technical Program Expanded Abstracts.1835-1839. https://doi.org/10.1190/1.3513199.

Reid, A.B., Allsop, J.M., Granser, H., Millet, A.J. and Somerton, I.W., (1990): Magnetic interpretations in three dimensions using Euler deconvolution Geophysics, 55, 80-91.

Roest, W. R., Verhoef, V., and Pilkington, M., (1992): "Magnetic interpretation using the 3-D analytic signal", Geophysics, v. 57, p. 116-125.

Riveros, K., Veloso, E. E., Campos, E., Menzies, A., and Véliz, W. (2014). Magnetic properties related to hydrothermal alteration processes at the Escondida porphyry copper deposit, northern Chile. Mineralium Deposita, 49(6), 693–707. https://doi.org/10.1007/S00126-014-0514-7

Salako, K. A., Adetona, A. A., Rafiu, A. A., Augie, A. I., Jimoh, M. O., Alkali, A., Muriana, R. A., and Lawrence, J. (2024). Integrated Geophysical Investigation for Gold Mineralization Potential over Southern Parts of Kebbi State and its Environs, Northwestern Nigeria. Heliyon, e34093. https://doi.org/10.1016/j.heliyon.2024.e34093

Schwarck, C., Salem, A., Chavanidis, K., Kirmizakis, P., and Soupios, P. (2025). Application of Euler Deconvolution to Magnetic Data for Mineral Exploration in the Arabian Shield. https://doi.org/10.2118/227120-ms

Salawu, N.B., Orosun, M.M., Adebiyi, L.S. (2020) Existence of subsurface structures from aeromagnetic data interpretation of the crustal architecture around Ibi, Middle Benue, Nigeria. SN Appl. Sci. 2, 427. https://doi.org/10.1007/s42452-020-2230-5

Shi, Y., Lesur, V., and Thébault, E. (2025). Characterizing the magnetic signal generated in the magnetosphere from 1996 to 2024 using ground geomagnetic data. https://doi.org/10.21203/rs.3.rs-7262458/v1

Soloviev, S. G., Kryazhev, S. G., and Seltmann, R. (2025). Geochemical fingerprints of the late Palaeozoic igneous rocks at the giant Muruntau gold deposit (Tien Shan, Uzbekistan) and implications for a metallogenic model. International Geology Review, 1-29. https://doi.org/10.1080/00206814.2025.2558016

Sternberg, L. (2023). Building geochemical vectors with trace element compositions of sulfides in orogenic gold mineral systems in northern Finland. Journal of Geochemical Exploration, 251, 107252. https://doi.org/10.1016/j.gexplo.2023.107252

Suleiman, U. (2025). Structural Interpretation of Aeromagnetic Data for Regional Controls on Gold Mineralization in Northwestern Nigeria. International Journal For Science Technology And Engineering, 13(9), 1796-1804. https://doi.org/10.22214/ijraset.2025.74298

Sun, Y., Yang, W., Zeng, X., and Zhang, Z. (2016). Edge enhancement of potential field data using spectral moments. Geophysics, 81(1). https://doi.org/10.1190/GEO2014-0430.1

Tapia, J., Townley, B., Córdova, L., Poblete, F., and Arriagada, C. (2016). Hydrothermal alteration and its effects on the magnetic properties of Los Pelambres, a large multistage porphyry copper deposit. Journal of Applied Geophysics, 132, 125-136. https://doi.org/10.1016/J.JAPPGEO.2016.07.005

Telford, W. M., Geldart, L. P., and Sheriff, R. E. (1990). Applied Geophysics. Cambridge University Press, second edition.

Thompson, D. T. (1982), EULDPH: A new technique for making computer-assisted depth estimates from magnetic data, Geophysics. 47, 31-37.

Tomlinson, K. M., Wilson, C. J. L., Hazeldene, R., and Lohe, E. M. (1988). Structural control on gold mineralization at Walhalla, Victoria. Australian Journal of Earth Sciences, 35(4), 421–444. https://doi.org/10.1080/08120098808729461

Tripp, G. I., and Vearncombe, J. R. (2004). Fault/fracture density and mineralization: a contouring method for targeting in gold exploration. Journal of Structural Geology, 26(6), 1087–1108. https://doi.org/10.1016/J.JSG.2003.11.002

Truswell JF, Cope RN (1963) The geology of parts of Niger and Zaria Provinces, Northern Nigeria. Geol Suvey Nigeria Bull 29:1–104

Turner DC (1983) Upper Proterozoic schist belts in the Nigerian sector of the Pan-African Province of West Africa. Precambrian Res 21:55–79

Tulepbayev, K., and Tulemissova, Z. S. (2025). Hydrothermal alteration and mineralogical zonation at the bozshakol porphyry copper deposit: integration of spectral, magnetic, and 3d modeling data. Ķazaķstan-Britan Tehnikalyķ Universitetìnìņ Habaršysy, 22(3), 356–369. https://doi.org/10.55452/1998-6688-2025-22-3-356-369

Ugwu, A. C., and Ekwueme, B. N. (2025). Tracing The Geologic Evolution Of Rocks In Ugep Southwest, Southeastern Nigeria: Evidence From Geochemical Signatures. Global Journal of Geological Sciences, 23(1), 49-59. https://doi.org/10.4314/gjgs.v23i1.4

Umaru, A.O., Okunlola, O., Danbatta, U.A. (2022) Litho-structural and hydrothermal alteration mapping for delineation of gold potential zones within Kaiama, northwestern Nigeria, using airborne magnetic and radiometric data. Arab J Geosci 15, 1771 . https://doi.org/10.1007/s12517-022-11048-8

Usman, A., Aku, M. O., Saleh, M. M., Lawan, A. M., and Momoh, K. O. (2025). Geochemical Characterization Of Gold and other Subtle Mineral Deposits in Parts of Maru Schist Belt Region of Zamfara State Northwestern Nigeria. https://doi.org/10.21203/rs.3.rs-7594899/v1

Wang, J., and Meng, X. (2019). Employing the bilateral filter to improve the derivative-based transforms for gravity and magnetic data sets. Studia Geophysica Et Geodaetica, 63(2), 215-228. https://doi.org/10.1007/S11200-018-0162-Y

Wang, Y., Wang, X., Suwen, J., Deng, B., Chen, Q., Xu, T., and Wang, Z. (2025). Geologically Guided Ambient Noise Tomography Inversion with 3D Interface Structures: Methodology and

Application to a Gold Mine Region in China. Geophysical Journal International. https://doi.org/10.1093/gji/ggaf376

Wright, J. B. (1985). Geology and mineral resources of West Africa. George Allen and Unwin, London. 187.

Wright, J. B., Hastings, D., Jones, W. B., and Williams, H.R. (1985). Geology and mineral resources of West Africa. George Allen and Urvin, London

Yang, X., Wu, J., and Xu, D. (2023). Application of integrated geological and structural investigations to the discovery of new mineral zones related to the Daping gold deposit, Southwest China. Ore Geology Reviews, 158, 105519. https://doi.org/10.1016/j.oregeorev.2023.105519

Yin, J., Li, K. Y., Shi, H., Yin, H., and Chao, Y. (2025). Mathematical, Physical, and Chemical Interpretations of Structural Control and Contributions to Gold Mineralization. https://doi.org/10.20944/preprints202501.1183.v1

Zaccarini, F., Baumgartner, R. J., Mavrogonatos, C., and Garuti, G. (2025). Magmatic significance and hydrothermal alteration of layered chromitites from the Bracco Gabbro Complex Ophiolite, Ligurian Ophiolites, Italy. Bulletin of the Mineral Research and Exploration, 178(178), 1–2. https://doi.org/10.19111/bulletinofmre.1764813

Zhao, C. (2023). Investigating Effects of Structural Deformation Regimes on Mineralization Distributions in Fluid-Saturated Rocks: Computational Simulation Approach through Generic Models. Minerals, 13(5), 664. https://doi.org/10.3390/min13050664